www.directivepublications.org

Journal of
Biosciences and Bioengineering

ISSN 2836-2535

Research Article

Ethics Approval Study On The Glucose Regulating Function Of Kudzu Resistant Starch Combined With Probiotics.

Wenting Jia[1], Shaojing Lin[1], Songjian Yuan[1], Haiyan Huang[1], Xiaomei Liu[1], Xiangman Ji[1], Bangzhou Zhang[1,2], Chuanxing Xiao[1,2*].

[1]School of Traditional Chinese Medicine, Fujian University of Traditional Chinese Medicine, Fuzhou, China.
[2]Center for Research and Development, Xiamen Treatgut Biotechnology Co., Ltd., Xiamen, China.

Running head: Kudzu resistant starch and probiotics in glucose regulation.

Abstract

Type 2 Diabetes Mellitus (T2DM) is a multifaceted metabolic disorder whose current treatments are limited by side effects and potential drug resistance. Recent studies highlight the gut microbiota's role in T2DM, with modulation via diet or probiotics showing potential for glycemic control. Kudzu resistant starch (KRS) and *Bifidobacterium adolescentis* are promising interventions, but their combined effects remain unexplored. This study investigates the synergistic effects of KRS and *Bifidobacterium adolescentis* TH02767 on glycemic control. *In vitro* fecal fermentation showed that KRS significantly enriched *Bifidobacterium* levels. In a T2DM mouse model, both KRS and *Bifidobacterium adolescentis* TH02767 decreased fasting blood glucose levels and enhanced glucose tolerance individually, and their combined treatment exhibited significantly enhanced therapeutic effects. These findings suggest that KRS and *Bifidobacterium adolescentis* could be a valuable strategy for developing functional foods targeting T2DM management, warranting further exploration of mechanisms and clinical applications.

Keywords : Kudzu Resistant Starch; *Bifidobacterium adolescentis*; Type 2 Diabetes Mellitus; Gut Microbiota; Glycolipid Metabolism.

INTRODUCTION

Type 2 Diabetes Mellitus (T2DM) is a complicated metabolic condition marked by persistent high blood glucose levels, resistance to insulin, and compromised insulin secretion (1). It has materialized as a health issue of global magnitude, affecting a considerable proportion of the populace and precipitating serious complications like cardiovascular diseases, kidney damage, and eye disorders (2,3). Currently, the treatment of T2DM mainly relies on oral hypoglycemic drugs or insulin Presently, the primary treatment modalities for T2DM involve the use of oral antidiabetic drugs or insulin injections (4). Although these methods can significantly reduce blood glucose levels in the short term, they also have some undeniable limitations. For example, they may be accompanied by side effects such as hypoglycemia and gastrointestinal discomfort, and long-term use of drugs may also lead to drug resistance in patients (5,6). Therefore, there is a pressing need to investigate additional therapeutic approaches. Notably, recent advances in microbiome research have revealed a novel and crucial player in the development and progression of T2DM: the gut microbiota (7). The human gut microbiota, comprising approximately 100 trillion microorganisms, is intricately involved in host metabolism, immune regulation, and overall health (8). Characterized by a reduction in beneficial bacteria and a rise in detrimental bacteria, gut microbiota dysbiosis has emerged as a defining feature of T2DM and is strongly linked to insulin resistance and disruptions in glucose metabolism (9,10).

Recent studies indicate that altering the gut microbiota via dietary changes or probiotic supplementation can not only enhance blood glucose regulation but also significantly reduce the risk of T2DM (11,12). For instance, dietary fibers and resistant starches (RS) have been shown to increase

***Corresponding Author:** Chuanxing Xiao, Center for Research and Development, Xiamen Treatgut Biotechnology Co., Ltd., Xiamen, China, **Tel:** 15960289801. **Email:** xiaoxx@treatgut.com
Received: 21-Mar-2025, Manuscript No. JOBB-4677 **; Editor Assigned:** 22-Mar-2025 **; Reviewed:** 12-Apr-2025, QC No. JOBB-4677 **; Published:** 26-Apr-2025, **DOI:** 10.52338/jobb.2025.4677
Citation: Chuanxing Xiao. Ethics approval Study on the glucose regulating function of kudzu resistant starch combined with probiotics. Journal of Biosciences and Bioengineering. 2025 April; 10(1). doi: 10.52338/jobb.2025.4677.

the abundance of beneficial bacteria, while also promoting the production of short-chain fatty acids (SCFAs), thereby improving insulin sensitivity (13). Probiotics, particularly strains of *Bifidobacterium*, have also demonstrated potential in regulating glucose metabolism and reducing inflammation (14,15).

In this context, Kudzu resistant starch (KRS), derived from the Kudzu plant, has emerged as a promising prebiotic. Recent studies have shown that KRS can improve glycemic control through multiple mechanisms, highlighting its promise as a potential therapeutic candidate for T2DM. One key mechanism involves the activation of the IRS-1/PI3K/AKT/Glut4 signaling pathway, which plays a crucial role in insulin-mediated glucose uptake and utilization (16). Additionally, KRS has been shown to modulate the gut microbiota composition by enriching beneficial bacteria such as *Bifidobacterium*, and enhancing the metabolic capabilities of the microbiota, thereby improving the intestinal microecology (17). Notably, similar to KRS, other forms of RS have been shown to reshape the gut microbiota composition by significantly increasing the abundance of beneficial bacteria such as *Bifidobacterium* (13). For instance, a recent study demonstrated that RS intervention led to an increase in *Bifidobacterium adolescentis* and other beneficial species, which were associated with improved metabolic outcomes, including reduced body weight and enhanced insulin sensitivity (18). Additionally, supplementation with *Bifidobacterium adolescentis* protected male mice from diet-induced obesity, highlighting the critical role of this bacterium in mediating the beneficial effects of RS (18,19). These findings support the feasibility of our study, suggesting that KRS may similarly modulate the gut microbiota to exert its glucose-regulating effects, as observed with other types of RS.

Current research has predominantly focused on the individual effects of these interventions, with limited exploration of their combined potential. Here we hypothesized that combining KRS with probiotics such as *Bifidobacterium adolescentis* may offer synergistic benefits in regulating glucose metabolism, as both interventions have been shown to independently improve metabolic health. Previous studies have suggested that combining prebiotics and probiotics can enhance their individual effects (20). Therefore, this study aims to investigate the combined glucose-regulating effects of KRS and *Bifidobacterium adolescentis* by examining their individual and combined impacts on the gut microbiota and glycemic control *in vitro* and in a T2DM mouse model. These insights could potentially lay the groundwork for the development of innovative functional foods and therapeutic approaches aimed at managing T2DM through modulation of the gut microbiota.

MATERIALS AND METHODS

Reagents

Kudzu powder was purchased from Hubei Gebaisheng Ge Ye Co., Ltd. MRS pre-made powder was obtained from Guangdong HuanKai Microbial Technology Co., Ltd. α-glucosidase, α-amylase, p-Nitrophenyl-α-D-glucopyranoside (pNPG), PBS buffer, and acarbose were sourced from Shanghai Yuanye Biotechnology Co., Ltd. Inulin and soluble starch were purchased from Shanghai Macklin Biochemical Co., Ltd. Na_2CO_3 was obtained from Xi Long Scientific Co., Ltd. DNS reagent and metformin were sourced from Beijing Solarbio Science & Technology Co., Ltd. DMEM culture medium was purchased from Wuhan Procell Life Science & Technology Co., Ltd. Trypsin-EDTA solution and CKK-8 kit were obtained from Shanghai Biyun Tian Biotechnology Co., Ltd. Glucose assay kit and glycogen assay kit were sourced from Nanjing Jiancheng Bioengineering Institute.

In vitro anaerobic dynamic fermentation using human fecal inocula

We conducted a preparation method of KRS by following the method reported by Song Xinqi et al. (16). Healthy donors are screened through questionnaires and physical examinations, and samples are collected with the informed consent of the participants. All donors, aged between 18 and 26 years, maintained their regular diet and had no history of gastrointestinal disorders or antibiotic use in the preceding three months. The fecal microbiota were extracted using an automated fecal microbiota extractor (model TG-01 Extn) from Xiamen Treatgut Biotechnology Co., Ltd. After centrifugation at 5000 g for 5 minutes, the extracted microbiota were resuspended in saline at a ratio of 1:1.1(21).

The *in vitro* fecal fermentation was conducted based on the method described by Lei et al. (22) with minor adaptations, and ethical approval was obtained from the Ethics Committee of the School of Medicine, Xiamen University (Ethics approval number: XDYX2022005). The composition of basic nutrient medium is shown in **Table S1**, and different carbon sources are added as fermentation medium according to experimental requirements. The fermentation solution was sterilized by autoclaving at 121°C for 15 minutes and adjusted to a pH of 7.0.

Table S1. Fermentation medium formulation.

Component	Concentration
Tryptone	10.0 g/L
Yeast Extract	5.0 g/L
NaCl	4.5 g/L
K_2HPO_4	0.5 g/L
KH_2PO_4	0.5 g/L
$MgSO_4 \cdot 7H_2O$	0.1 g/L
$CaCl_2 \cdot 2H_2O$	0.1 g/L
$NaHCO_3$	1.5 g/L
Peptone	2.5 g/L
Tween-80	1 mL/L
L-Cysteine	0.5 g/L
Resazurin	1 mg/L
Vitamin K_1	50 mg/L
Distilled Water	1000 mL
pH	6.5

PART I

10% of inoculum preparation were inoculated in fermentation medium under anaerobic aseptic system. The experimental design included four groups: control group (CON), 0.5% KRS group (KRS-0.5), 1% KRS group (KRS-1) and 3% KRS group (KRS-3). Three parallel experimental groups were set up for each group, with tubes containing 0.5% or 1% or 3% w/v KRS as the carbon source.

PART II

10% of inoculum preparation were inoculated in fermentation medium under anaerobic aseptic system. Determine the optimal concentration according to part I. The experimental design included three groups: control group (CON), 0.5% KRS group (KRS) and 0.5% inulin group (POS). For each experimental condition, three replicate groups were established, using tubes that contained 0.5% KRS and inulin (w/v) as the carbon source.

The samples were cultured at 37°C in an anaerobic shaking incubator maintained at a constant temperature, set at 200 rpm. Following 24 hours of fermentation, the fermentation broth was harvested and subjected to centrifugation at 5000 g for 5 minutes. Subsequently, the 16S rDNA sequencing was performed on the collected samples.

Preparation of strain samples

A total of over 30 strains of *Bifidobacterium* were obtained from the strain library of Xiamen Treatgut Biotechnology Co., Ltd. These strains were retrieved from storage at -80°C, activated, and subsequently purified through three consecutive subcultures to obtain pure single colonies. The inhibitory activities of α-glucosidase and α-amylase, as well as the anti-diabetic effects on IR-HepG2 cells, were measured using Cell-free supernatant (CFS) and Intracellular cell-free extract (CFE) prepared according to the method of Zhang et al. (23).

Inhibition of α-glucosidase and α-amylase activity

The α-glucosidase and α-amylase assays were performed according to the method of Kim et al. (24), with modifications.

A mixture of 500 μL CFS from the isolates and an equal volume of PBS (0.2 M, pH 7.0) containing α-amylase (4 U/mL, pH 7.0) was incubated at 37°C for 10 minutes. Next, 500 μL of 1% starch solution was added, and the mixture was left to incubate for another 10 minutes at 37°C. The process was concluded by introducing 1 mL of DNS reagent and placing it in a boiling water bath for 5 minutes. The absorbance was measured at 540 nm to evaluate α-amylase inhibition after the solution was cooled to room temperature and diluted with water.

The α-amylase inhibition rate(%) can be calculated from the fluorescence readings defined above using Eq. 1.

$$\alpha\text{-amylase inhibition rate}(\%)=1-\frac{A540(Sample)-A540(Blank\ sample)}{A540(Control)} \quad (1)$$

where A540 represents the absorbance value at 540 nm, Control is the absorbance of the control group without the tested sample, Sample is the absorbance of the tested sample group, and Blank Sample is the absorbance of the control group without the enzyme.

For the α-glucosidase assay, a mixture of 25 μL CFS, 25 μL PBS (0.2 M, pH 7.0) and 50 μL 1.5 mM pNPG was pre-incubated at 37°C for 10 minutes. Next, 30 μL of α-glucosidase (0.2 U/mL) was added, followed by an additional 30-minute incubation at 37°C. To determine the percent inhibition, the reaction was stopped with 50 μL of Na_2CO_3(0.1 M), and the absorbance of 4-nitrophenol was measured at 405 nm.

The α-glucosidase inhibition rate(%) can be calculated from the fluorescence readings defined above using Eq. 2.

$$\alpha\text{-glucosidase inhibition rate}(\%)=1-\frac{A405(Sample)-A405(Blank\ sample)}{A405(Control)-A405(Blank\ control)} \quad (2)$$

where A405 represents the absorbance value at 405 nm, Control is the absorbance of the control sample without the tested sample, Blank Control is the absorbance of the control sample without the tested sample and enzyme, Sample is the absorbance of the tested sample, and Blank Sample is the absorbance of the control sample without the enzyme.

The IR-HepG2 cell model for antidiabetic test

The HepG2 cells, sourced from Xiamen University, were cultured at 37°C in an incubator with 5% CO_2, using DMEM medium. After reaching 80% confluence, the cells were digested using 0.25% trypsin and passaged, and cells in the logarithmic growth phase were picked for subsequent experiments. The experimental methods followed the approach outlined by Huang et al. (25). Logarithmic phase HepG2 cells were seeded at a density of 1×10^5 cells/mL in 96-well plates. After cell attachment, the old culture medium was removed, and the cells were starved for 10 hours with serum-free medium. Subsequently, the cells were treated with basal medium containing different concentrations of insulin for 24 and 48 hours. Additionally, cells were also treated with varying concentrations of metformin to determine the optimal dose of the positive control drug. Cell viability was assessed using the CCK-8 assay. Ten microliters of CCK-8 solution was added to each well, and the plate was incubated for 1.5 hours in the incubator. Absorbance was then read at 450 nm.

The cell viability (%) can be calculated from the absorbance readings using Eq. 3:

$$cell\ viability(\%)=\frac{A450(Sample)}{A450(Control)} \quad (3)$$

where A450 represents the absorbance value at 450 nm, Control is the absorbance of the control group, and Sample is the absorbance of the sample group.

The glucose uptake was determined with the glucose assay kit, and the glucose consumption of different insulin concentrations under different action time was calculated to determine the experimental conditions for the construction of IR-HepG2 Cell Model.

The glucose uptake (mmol/L) can be calculated from the absorbance readings using Eq. 4:

$$glucose\ uptake\ (mmol/L)=G0-Gx \quad (4)$$

Where G0 is the glucose concentration (mmol/L) in the blank control group without cells, and Gx is the measured glucose concentration (mmol/L) in the culture medium of sample group.

After the establishment of IR-HepG2 Cell Model, the effects of CFS and CFE on the activity of IR-HepG2 Cell Model, glucose uptake and glycogen content were evaluated in turn. Glycogen assay using a glycogen assay kit.

The glycogen content (mmol/L) can be calculated from the absorbance readings using Eq. 5:

$$\text{glycogen content (mmol/L)} = \frac{A620(\text{Sample})}{A620(\text{Standard})} \times C \times 10 \div 1.1 \times V \quad (5)$$

where A620 represents the absorbance value at 620 nm, Sample is the absorbance of the sample group, Standard is the absorbance of the standard sample, C is the concentration of the standard sample (0.01 mg/mL), and V is the volume of the sample (0.5 mL).

Validation of the Effects of KRS on Bacterial Growth

To investigate the effects of KRS on bacterial growth, different concentrations of KRS (0%, 0.125%, 0.25%, 0.5%, 1%, and 2%) were added to MRS liquid medium. The medium was sterilized at 121°C for 15 minutes after KRS addition, and KRS samples were sterilized using UV irradiation before incorporation. The experimental procedures were performed according to the method of Amarnath et al. (26).

Promotive Effects on Hypoglycemic Bacteria; Bacterial cultures activated for three generations were adjusted to an OD_{600} value of 1.0 and inoculated into the medium at 2% (v/v). After anaerobic incubation at 37°C for 24 hours, the OD_{600} values were measured to assess bacterial growth promotion compared to the blank control group without KRS.

Inhibitory Effects on Pathogenic Bacteria: Similarly, bacterial cultures activated for three generations were adjusted to an OD_{600} value of 1.0 and inoculated into the medium at 2% (v/v). After anaerobic incubation at 37°C for 4 hours, the OD_{600} values were measured to evaluate bacterial growth inhibition compared to the blank control group without KRS.

Animal and experimental design

Six-week-old male SPF-grade C57BL/6J mice were obtained from Guangdong Yaokang Biotechnology Co., Ltd. (Certificate No. SCXK [Yue] 2023-0067). Mice were maintained at 22 ± 2°C 60% ± 10% relative humidity, under a 12-hour light/dark cycle with free access to food and water. Approval for the study was granted by the Animal Ethics Committee of the Second Affiliated Hospital of Fujian University of Traditional Chinese Medicine (Approval No.: FJPSPH-IAEC2024110).

After a one-week adaptation period, the mice were split into two groups: the normal control (CON) group received a standard diet (Cat#: XTCON50J), whereas the other 50 mice were given a diet consisting of 60% high fat (Cat#: XTHF60). Following a four-week feeding regimen, mice on a high-fat diet were intraperitoneally injected with STZ (40 mg/kg) for five days straight, while the CON group was given just citrate buffer. One week after the injections, tail blood was collected to measure fasting blood glucose (FBG), and mice with FBG > 11.1 mmol/L were classified as having T2DM. The experimental procedures were performed according to the method of Yu et al. (27).

In the sixth week, diabetic mice were treated daily via gavage with normal saline (MOD), metformin (200 mg/kg in saline, MET), KRS (4.5 g/kg in saline, KRS), *Bifidobacterium adolescentis* TH02767 suspension (1×10^9 CFU/mL, PRO), or a combination of KRS and *Bifidobacterium adolescentis* TH02767 (MIX). Body weight and FBG were monitored weekly. After 4 weeks, mice were euthanized by eye enucleation. Biochemical analysis and ELISA assays were conducted on collected blood samples. Liver and pancreas tissues were harvested for H&E staining, and cecal contents were gathered for 16S rDNA sequencing. All samples were kept at -80°C until analysis.

Determination of glycemic and lipid metabolic parameters

To assess the metabolic status of mice, various glycemic and lipid parameters were measured. Weekly monitoring of body weight and FBG levels was conducted using a glucometer (Yuwell) through tail-tip blood sampling. A week prior to the conclusion of the treatment, an oral glucose tolerance test (OGTT) was conducted. An OGTT was performed one week before the end of treatment. Mice were fasted overnight for 12 hours and then administered a glucose solution (2 g/kg) orally. To assess OGTT, blood glucose levels were recorded at 0, 15, 30, 60, 90, and 120 minutes after glucose was given, and the area under the curve (AUC) was computed.

At the end of the 4-week intervention, mice were euthanized, and blood was collected for analysis. Serum was obtained by centrifugation (8000 rpm, 5 min) after clotting at room temperature for 4 hours. Levels of glycated hemoglobin A1c (HbA1c), serum insulin (INS), total cholesterol (TC), triglycerides (TG), low-density lipoprotein cholesterol (LDL-C), high-density lipoprotein cholesterol (HDL-C), aspartate aminotransferase (AST), and alanine transaminase (ALT) were measured using an automated biochemical analyzer. The reagents for the biochemical analyzer were purchased from Shenzhen Mindray Bio-Medical Electronics Co., Ltd. Levels of tumor necrosis factor-α (TNF-α), interleukin-1β (IL-1β), interleukin-10 (IL-10), interleukin-6 (IL-6)were quantified using ELISA. The ELISA kits were purchased from (Ruixinbio Quanzhou, china) Ouanzhou Ruixin Biological TechnologyCo., LTD Quanzhou,china.

Statistical Analysis All data were shown as means ± standard deviation (means ± s.d.). Data processing and graphing were performed using GraphPad Prism 7, while statistical analyses were conducted using SPSS Statistics 25.0. Depending on the experimental design and data characteristics, either t-tests or one-way ANOVA were used to assess significant differences. For t-tests, $P < 0.05$was considered statistically significant. For one-way ANOVA, differences were considered significant if

marked by different letters.

RESULTS AND DISCUSSION

***In vitro* anaerobic dynamic fermentation using human fecal inocula. KRS** significantly enhanced gut microbiota diversity and abundance. Compared to the control, Shannon and Simpson indices increased in KRS groups. β-Diversity analysis revealed distinct differences between KRS and CON groups, indicating structural changes in the microbial community. At the phylum level, KRS groups increased Firmicutes and Actinobacteriota while reducing Proteobacteria and Bacteroidetes **(Fig. S1)**. At the genus level, KRS groups significantly enriched beneficial genera such as *Bifidobacterium* and *Faecalibacterium* ($P < 0.05$), while suppressing *Escherichia-Shigella*. The 0.5% KRS group achieved the highest enrichment of *Bifidobacterium*, demonstrating its optimal prebiotic effect **(Fig. 1A and B)**. Therefore, 0.5% KRS was selected for subsequent experiments due to its significant health-promoting potential.

Figure S1. Effects of different concentrations of KRS on gut microbiota. (A) α diversity of gut microbiota under different concentrations of KRS. (B) β diversity of gut microbiota under different concentrations of KRS. (C) Composition of gut microbiota at the phylum level under KRS and inulin treatments.

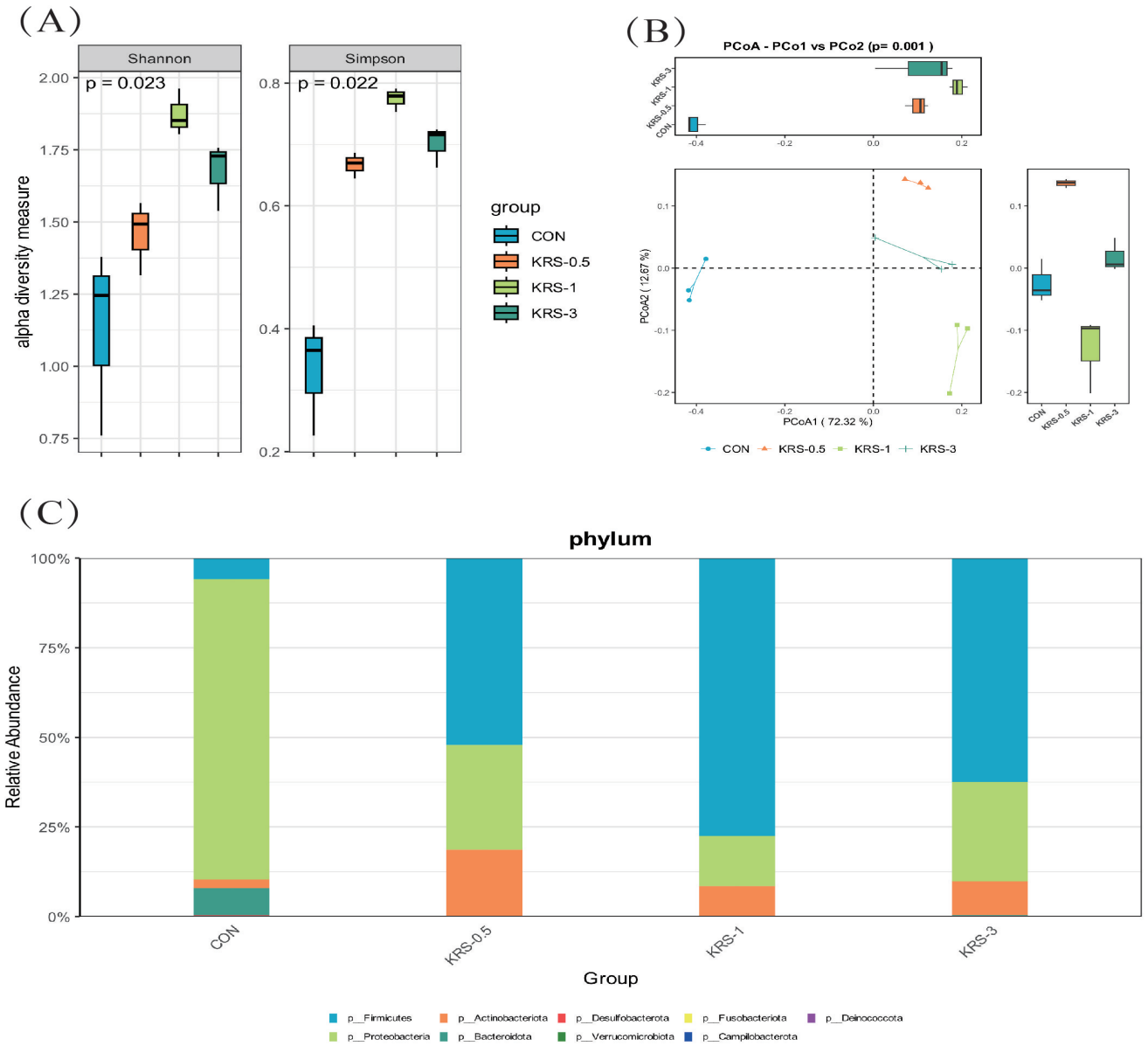

Figure 1. Effects of KRS on gut microbiota. (A) Composition of gut microbiota at the genus level under different concentrations of KRS. (B) Differential analysis of gut microbiota at the genus level under different concentrations of KRS. (C) Composition of gut microbiota at the genus level under KRS and inulin treatments. (D) Differential analysis of gut microbiota at the genus level under KRS and inulin treatments. (E) Differential analysis of *Bifidobacterium* at the genus level.

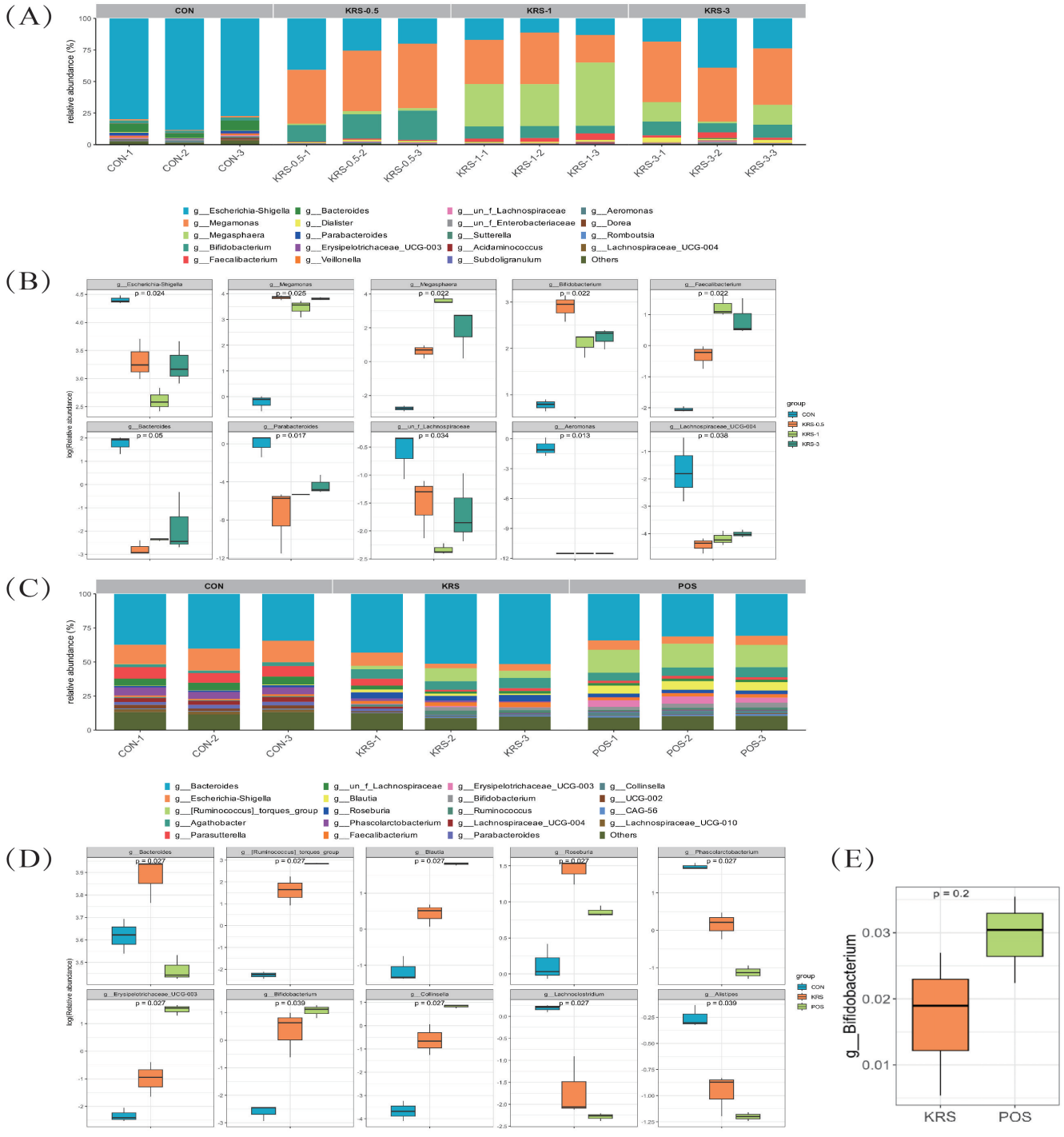

When repeated with inulin as a control, α-diversity analysis revealed no notable differences in Shannon and Simpson indices among the CON, KRS, and POS groups **(Fig. S2A)**. However, β-diversity analysis revealed significant differences between the KRS and POS groups compared to the CON group **(Fig. S2B)**, suggesting that both KRS and inulin could modulate gut microbiota structure. At the phylum level, KRS group increased Bacteroidota, Firmicutes, and Actinobacteriota, while inulin increased Firmicutes and Actinobacteriota **(Fig. S2C)**. At the genus level, both the KRS and POS groups significantly enhanced the abundance of beneficial genera, including *Bacteroides, Blautia*, and *Bifidobacterium* ($P < 0.05$), with no significant difference in *Bifidobacterium* enrichment between them **(Fig. 1C-E)**. This result aligns with Zhao et al.'s study (28), which demonstrated that lentil resistant starch promotes beneficial gut bacteria growth while inhibiting harmful ones. Specifically, KRS significantly

increases the abundance of beneficial *Bifidobacterium* while inhibiting harmful bacteria, thereby exhibiting notable prebiotic properties. These outcomes point to the potential of KRS as a functional ingredient in adjusting gut microbiota composition and boosting gut health.

Figure S2. Comparative effects of KRS and inulin on gut microbiota. (A) α diversity of gut microbiota under different concentrations of KRS. (B) β diversity of gut microbiota under different concentrations of KRS. (C) Composition of gut microbiota at the phylum level under KRS and inulin treatments.

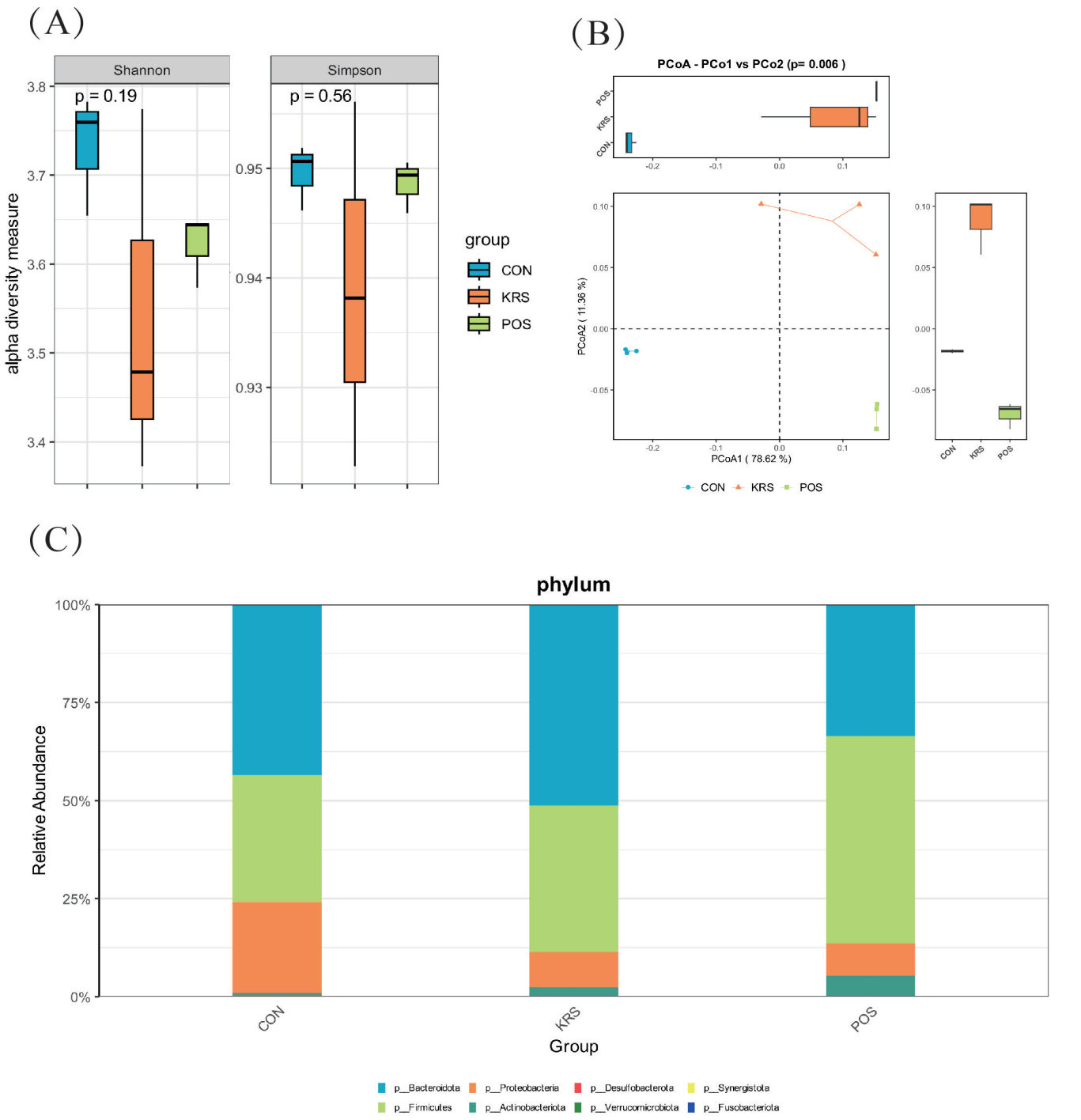

Inhibition of α-glucosidase and α-amylase activity

In carbohydrate metabolism, α-glucosidase and α-amylase break down carbohydrates into glucose. Inhibiting these enzymes delays glucose release, reducing postprandial blood glucose spikes, which is crucial for diabetes management (29). In this study, the α-glucosidase inhibitory activities of 32 strains were investigated to identify strains with potential hypoglycemic activity. Acarbose (an antidiabetic drug) and *Lacticaseibacillus rhamnosus* GG (LGG), known to have an antidiabetic effect, were used as positive controls. The inhibitory rates of α-glucosidase and α-amylase by the supernatants of each strain are shown in

Figures 2, respectively. Compared with the standard strain LGG, four strains of *Bifidobacterium* (TH02767, TH02869, TH03934, and TH04209) showed significantly higher inhibitory effects on both α-glucosidase and α-amylase than LGG ($P < 0.05$) **(Table 1)**. These findings indicate that the selected *Bifidobacterium* strains have strong potential for hypoglycemic effects and could serve as promising probiotic candidates for diabetes management.

Figure 2. Inhibition rates of α-glucosidase and α-amylase. (A) Inhibition rate of α-glucosidase. (B) Inhibition rate of α-amylase. Data are expressed as means ± standard deviation (n = 3). Asterisks indicate significant differences using Dunnett's test. *P < 0.05, **P < 0.01 (vs. standard strain LGG).

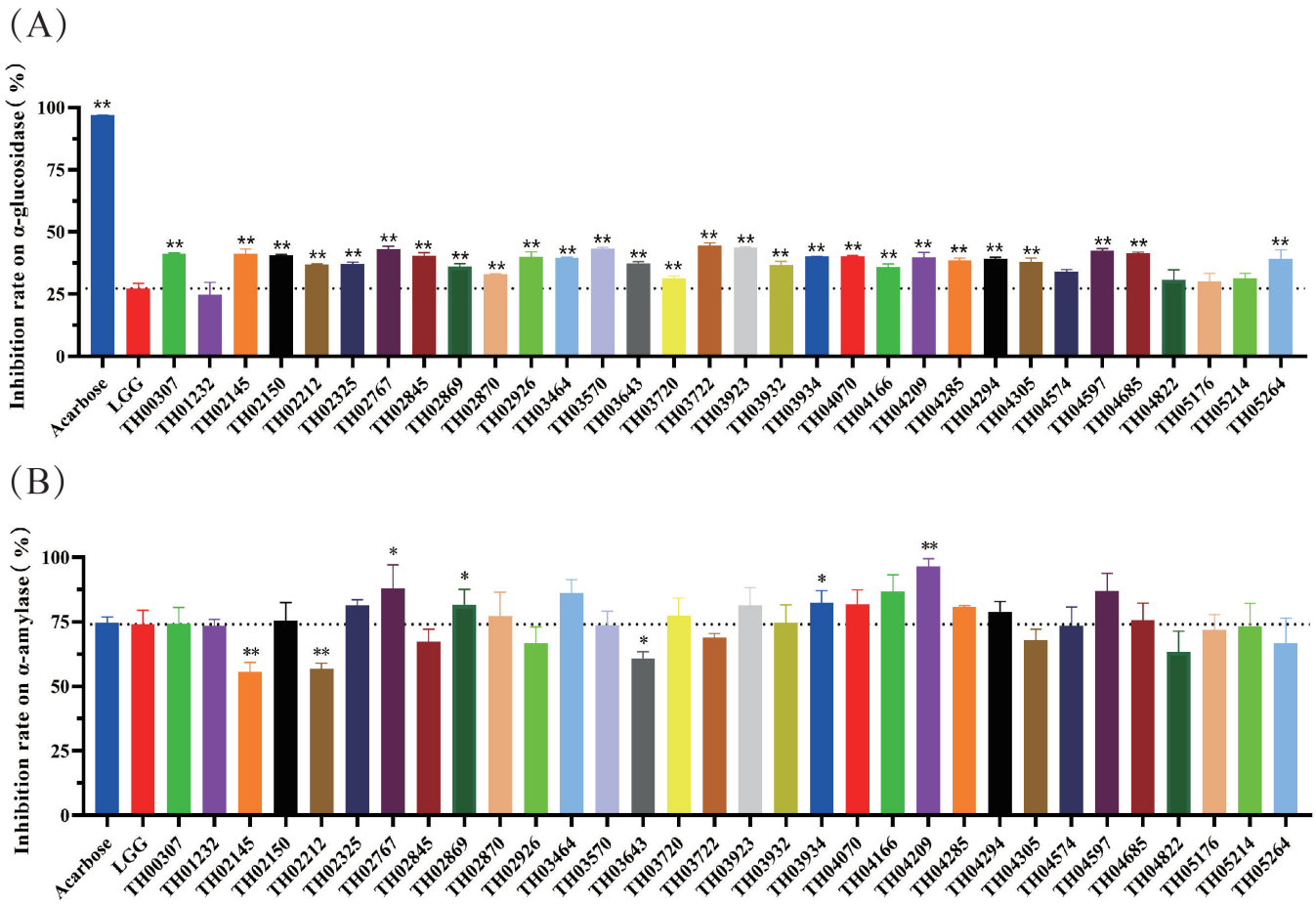

Table 1. Candidate hypoglycemic bacteria with inhibitory effects on both α-glucosidase and α-amylase.

Strain No.	Bacterial species	α-glucosidase inhibition rate (%)	α-amylase inhibition rate (%)
LGG	*Lactobacillus rhamnosus*	27.25±2.11	74.07±5.40
TH02767	*Bifidobacterium adolescentis*	43.19±1.12	86.99±3.61
TH02869	*Bifidobacterium longum subsp. longum*	36.21±1.08	84.89±2.13
TH03934	*Bifidobacterium breve*	40.12±0.21	88.69±2.82
TH04209	*Bifidobacterium bifidum*	39.80±1.99	96.32±3.12

Data were expressed as means ± standard deviation (n = 3).

The IR-HepG2 cell model for antidiabetic test

Based on the experimental results, HepG2 cells were exposed to 1×10^{-6} mol/L insulin for 48 hours to establish the IR-HepG2 cell model, using 4 mM metformin as the positive control. Different concentrations of CFS or CFE from various bacterial strains were used to treat IR-HepG2 cells, with no notable cytotoxicity observed **(Fig. S3).**

Figure S3. Preliminary experiments for establishing the IR-HepG2 cell model. (A) Effects of different concentrations of insulin on HepG2 cell viability. (B) Effects of different concentrations of insulin on glucose consumption in HepG2 cells. (C) Effects of different concentrations of metformin on HepG2 cell viability. (D) Effects of various strains' CFS on viability of IR-HepG2 cells. (E) Effects of various strains' CFE on viability of IR-HepG2 cells. Data are expressed as means ± standard deviation (n = 3). Asterisks indicate significant differences using Dunnett's test. *P < 0.05, **P < 0.01 (vs. MOD group).

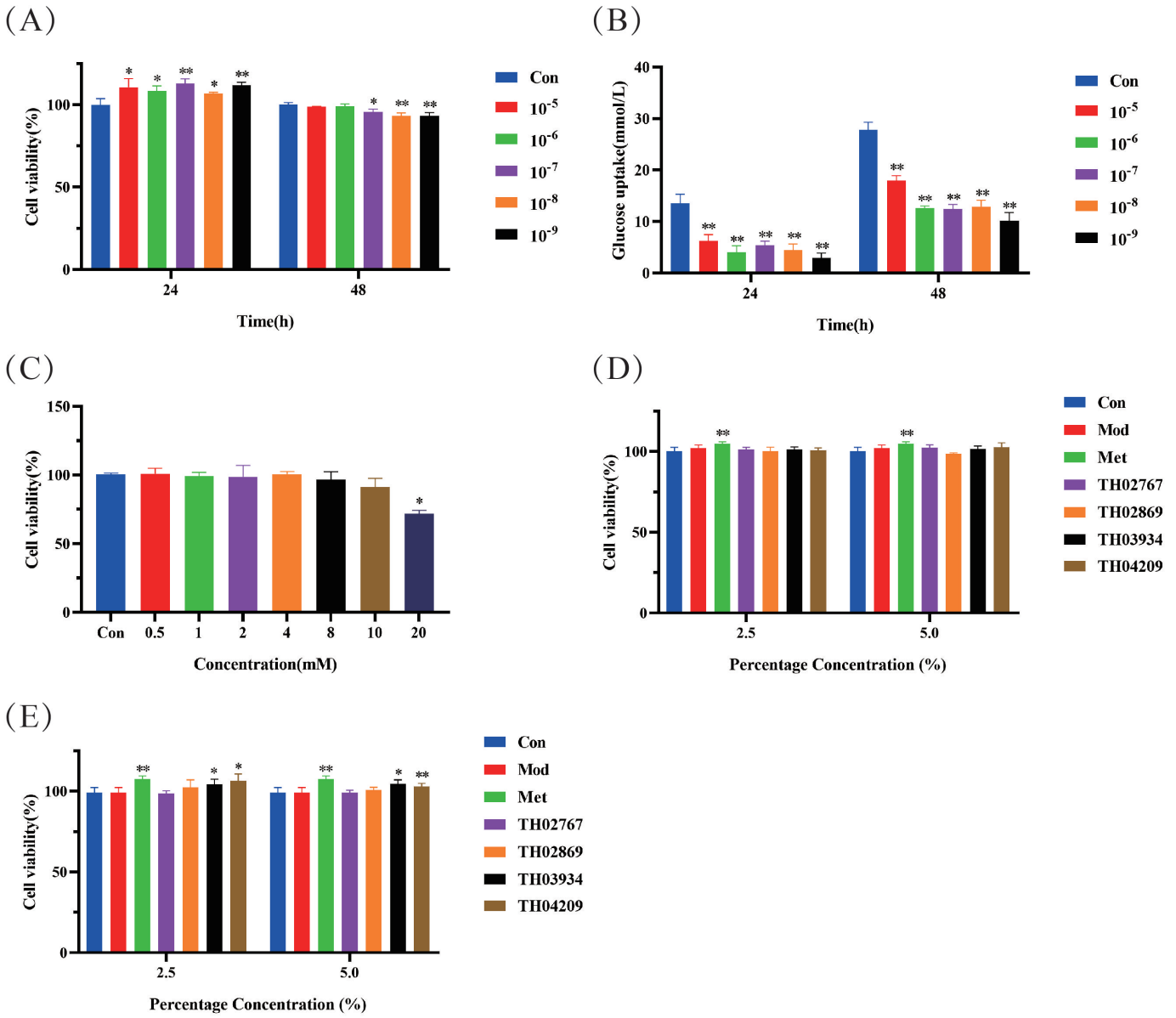

Our study demonstrated that the tested bacterial strains significantly modulated glucose uptake and glycogen content in IR-HepG2 cells, as shown in **Figure 3**. At a concentration of 2.5%, the CFS of strains TH02767 and TH02869 markedly increased glucose consumption (P < 0.01), while strains TH03934 and TH04209 showed significant effects (P < 0.05). At 5%, strains TH02767 and TH02869 maintained significant effects (P < 0.01), with TH04209 also showing significance (P < 0.05). For CFE, strains TH03934 and TH04209 significantly enhanced glucose uptake at 2.5% (P < 0.05), and strains TH02767 and TH04209 did so at 5% (P < 0.05).

Figure 3. The IR-HepG2 Cell Model for antidiabetic test. (A) The effect of different concentrations of bacterial cell-free extracts on glucose consumption in IR-HepG2 cells. (B) The effect of different concentrations of bacterial supernatants on glucose consumption in IR-HepG2 cells. (C) The effect of different concentrations of bacterial cell-free extracts on glycogen synthesis in IR-HepG2 cells. (D) The effect of different concentrations of bacterial supernatants on glycogen synthesis in IR-HepG2 cells. Data are expressed as means ± standard deviation (n = 3). Asterisks indicate significant differences using Dunnett's test. *P < 0.05, **P < 0.01 (vs. MOD group). Hashes indicate significant differences using Dunnett's test. $^{\#}P$< 0.05, $^{\#\#}P$ < 0.01 (vs. CON group).

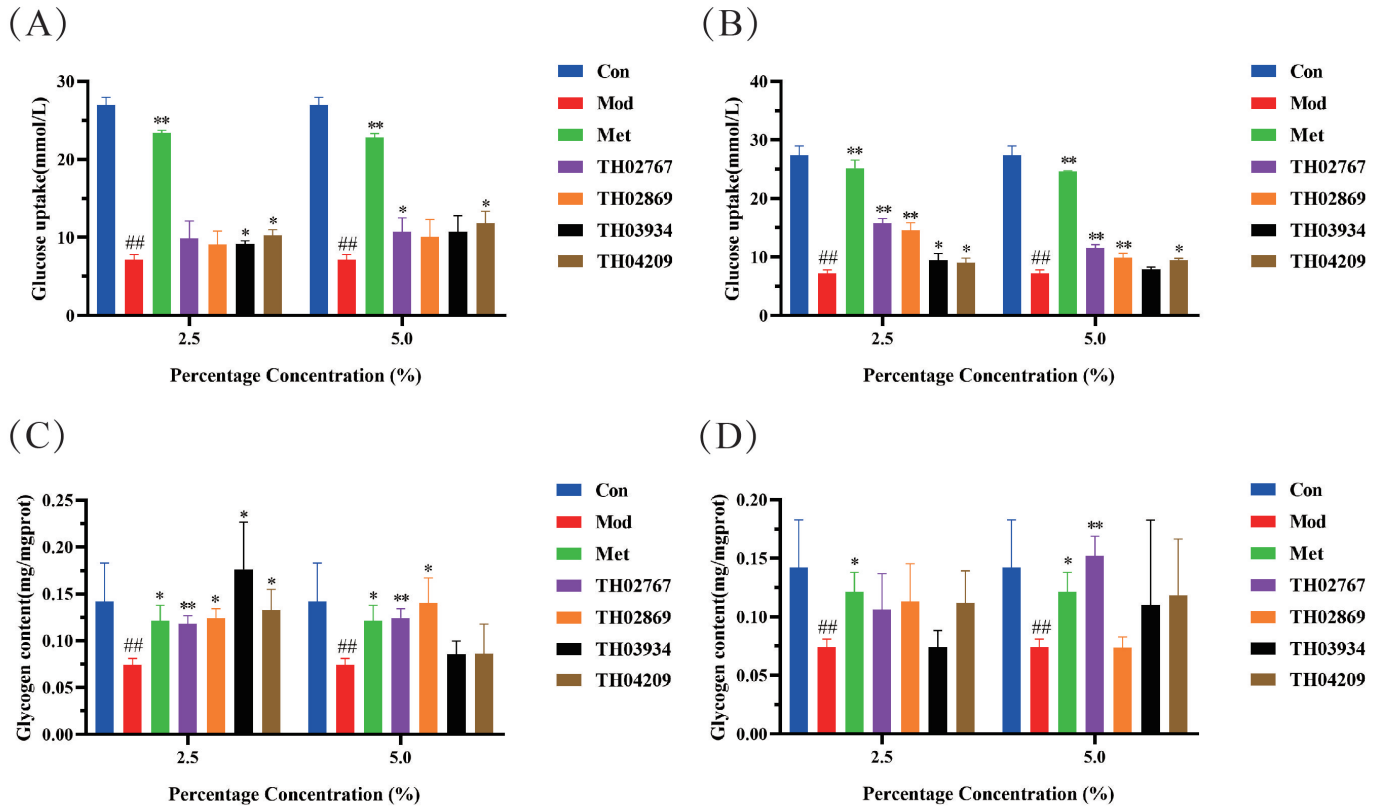

Regarding glycogen content, at 2.5%, only CFS of strain TH02767 significantly increased glycogen levels (P < 0.01). At 5%, strains TH0286 and TH02767 showed significant and highly significant effects, respectively (P < 0.05). For CFE, strains TH02869, TH03934, and TH04209 significantly enhanced glycogen content at 2.5% (P < 0.05), with TH02767 showing a highly significant effect (P < 0.01).

The results suggest that the metabolic products of these *Bifidobacterium* strains have significant potential to regulate cellular glucose metabolism, with notable strain-specific and concentration-dependent effects. Their ability to enhance glucose uptake and increase glycogen content indicates a potential to significantly improve metabolic function in insulin-resistant cells (30).

Validation of the effects of KRS on bacterial growth

After 24 hours of co-culture with four hypoglycemic bacterial strains, KRS significantly promoted the proliferation of strain TH02767, especially at a concentration of 0.25%, where its OD_{600} value was significantly higher than other groups (P < 0.05). This suggests that KRS, as a prebiotic, can enhance the growth of beneficial gut bacteria such as *Bifidobacterium adolescentis*, potentially through selective fermentation that leads to the production of short-chain fatty acids (SCFAs) that support gut health **(Fig. 4A)**.

After 4 hours of co-culture with four pathogenic bacteria, KRS significantly inhibited the growth of *Escherichia coli* and *Staphylococcus aureus*, with their OD_{600} values inversely related to KRS concentration. At 2% concentration, the OD_{600} values were significantly lower than other groups (P < 0.05). For *Staphylococcus epidermidis*, OD_{600} was significantly lower at 0.5% KRS concentration (P < 0.05), while *Staphylococcus citreus* showed significant inhibition at both 0.5% and 1.0% KRS concentrations (P < 0.05). These results indicate that KRS can selectively inhibit the growth of pathogenic bacteria, further supporting its potential as a prebiotic **(Fig. 4B)**.

Figure 4. Impact of KRS on Bacterial Strains: Promotion and Inhibition. (A) Promotive effects of KRS on the proliferation of potential hypoglycemic bacterial strains. (B) Inhibitory effects of KRS on the growth of pathogenic bacterial strains. Data are expressed as means ± standard deviation (n = 3). Letters indicate significant differences using one-way ANOVA followed by Tukey's HSD test, means with different letters are significantly different ($P < 0.05$).

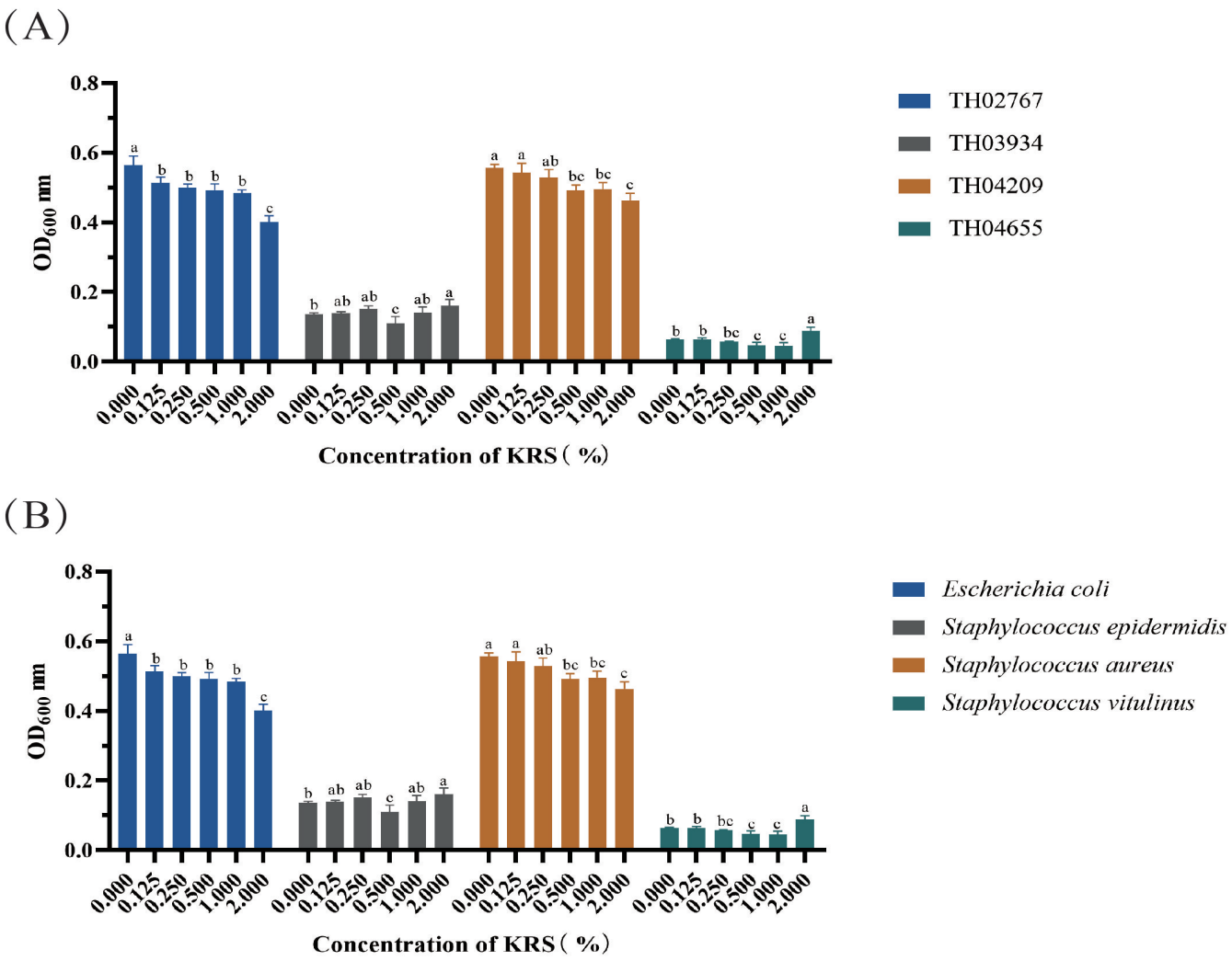

Our findings that KRS significantly promotes the growth of beneficial *Bifidobacterium adolescentis* TH02767 while inhibiting pathogenic bacteria such as *Escherichia coli* are consistent with the study by Qu et al. (31), who demonstrated that medicinal polysaccharides have the ability to selectively boost the growth of specific gut bacterial strains. This aligns with our earlier *in vitro* simulated fermentation experiments, further confirming the potential prebiotic properties of KRS in modulating the structure and function of the gut microbiota by increasing beneficial bacteria and inhibiting harmful ones.

Animal experiments

The animal experimental procedure is depicted in **Figure 5**. The high-fat diet combined with STZ successfully induced obesity and elevated glucose levels in mice, thereby establishing a T2DM mouse model. After drug administration, both positive and probiotic interventions significantly reduced the body weight of mice **(Figure 6A, Table 2)**. All intervention groups significantly improved hyperglycemia induced by high-fat diet combined with STZ. The combination group showed the best hypoglycemic effect, comparable to the positive group, suggesting that the combined intervention of KRS and probiotics may exert a more significant hypoglycemic effect through synergistic action **(Figure 6B, Table 3)**. In terms of oral glucose tolerance **(Figure 6C)**, the AUC of the OGTT was significantly elevated in MOD group compared with CON group ($P < 0.01$), indicating impaired glucose tolerance. Except for the probiotic group, the AUC values of MET, KRS, and MIX groups were all significantly lower than that of MOD group ($P < 0.05$), suggesting improved glucose tolerance. In terms of HbA1c **(Figure 6D)**, only MET group showed a significant decrease compared with MOD group, while no significant differences were observed in the other intervention groups. These results indicate that both KRS and probiotics have some capacity to regulate blood glucose levels, but their

effects on long-term glycemic control are weaker than those of the positive control drug, metformin. The results of the four lipid parameters showed that, compared with CON group, the levels of TC, TG, lDL-C, and HDL-C in MOD group were significantly elevated ($P < 0.01$). However, there was no notable reduction in the levels of the four blood parameters across any groups **(Figure S4)**. This result indicates that the interventions had limited effects on regulating lipid metabolism. As for serum insulin levels **(Figure 7A)**, MOD group had much higher insulin levels than CON group ($P < 0.01$), indicating pancreatic cell damage and impaired insulin secretion function due to the modeling process. After intervention, insulin levels in all treatment groups were significantly reduced ($P < 0.01$), with the most notable decreases observed in the MET and MIX groups. To determine the hypoglycemic effects of KRS and probiotics, we performed H&E staining analysis. H&E staining of the pancreas was employed to assess pathological changes such as inflammation, acinar necrosis, and overall pancreatic damage. MOD group exhibited structural and functional damage of the pancreatic islet cells. Compared to the MOD group, PRO group showed some degree of improvement but still had varying degrees of islet cell atrophy and irregular islet shapes, KRS and MIX group had clearer islet boundaries, tighter islet cell arrangement, and improved islet morphology, which were comparable to MET group**(Figure 7B)**. The presence of steatosis and lipid accumulation in liver tissue was determined through H&E staining, and liver function was evaluated with ALT and AST. Severe steatosis developed in MOD group, resulting in significant elevations of AST and ALT in the liver. Compared to MOD group, PRO group showed no significant improvement, KRS group exhibited a significant reduction in vacuolar degeneration and steatosis, MIX and MET groups showed marked alleviation of pathological changes, with hepatocyte morphology closely resembling that of CON group, cells were round and plump, with tight arrangement and no obvious inflammatory cell infiltration **(Figure 7D)**. Compared with MOD group, the levels of ALT and AST in all intervention groups decreased but did not reach significant differences **(Figure 7C)**, indicating that the interventions had some beneficial effects but might not be sufficient to fully repair liver damage in the short term.

Figure 5. Schematic representation of the experimental procedure.

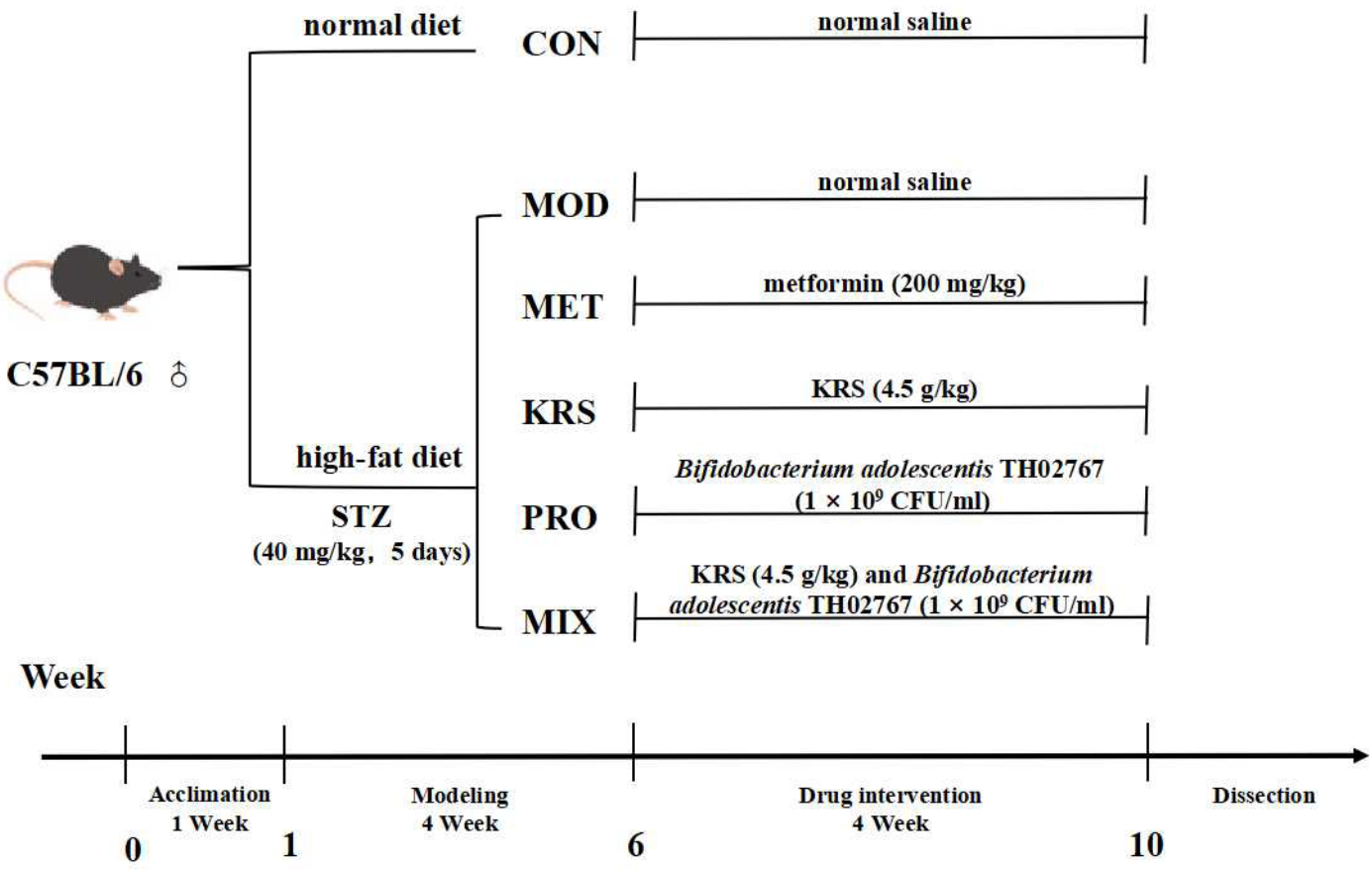

Figure 6. Assessment of Antidiabetic Efficacy through Metabolic Parameters in T2DM Mice. (A) Body weight of each group of mice. (B)FBG levels in each group of mice. (C) Area under the curve of the OGTT in each group of mice. (D) HbA1c levels in each group of mice. Data are expressed as means ± standard deviation (n = 10). Asterisks indicate significant differences using Dunnett's test. *P < 0.05, **P < 0.01 (vs. MOD group). Hashes indicate significant differences using Dunnett's test. $^{\#}P$< 0.05, $^{\#\#}P$ < 0.01 (vs. CON group).

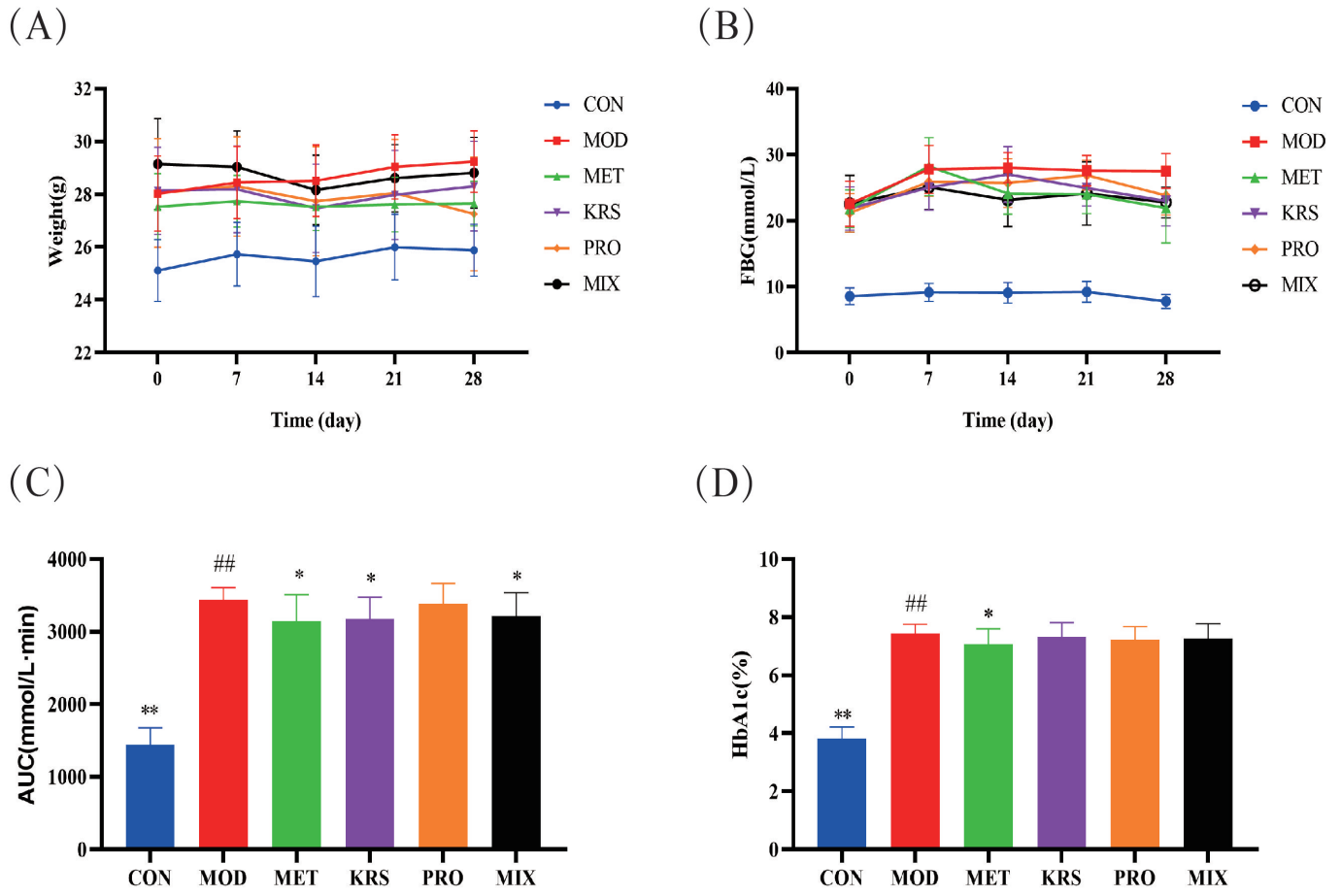

Table 2. Effect of KRS and probiotics on body weight of T2DM mice.

Group name	0 week (g)	1 week (g)	2 week (g)	3 week (g)	4 week (g)
CON	25.11±1.1	25.73±1.14	25.46±1.26	26.00±1.17	26.60±1.20
MOD	28.03±1.35$^{\#\#}$	28.45±1.3$^{\#\#}$	28.51±1.28$^{\#\#}$	29.04±1.15$^{\#\#}$	29.24±1.11$^{\#\#}$
MET	27.53±1.18	27.73±0.92	27.53±0.84	27.61±0.98*	27.65±0.80**
KRS	28.13±1.56	28.19±1.56	27.47±1.59	27.98±1.60	28.31±1.61
PRO	28.06±1.95	28.30±1.78	27.74±1.96	28.05±1.93	27.25±2.04*
MIX	29.15±1.63	29.03±1.29	28.16±1.25	28.61±1.21	28.82±1.27

Data were expressed as means ± standard deviation (n = 10). Asterisks indicate significant differences using Dunnett's test. *P < 0.05, **P < 0.01 (vs. MOD group). Hashes indicate significant differences using Dunnett's test. $^{\#}P$< 0.05, $^{\#\#}P$ < 0.01 (vs. CON group

Table 3. Effect of KRS and probiotics on FBG of T2DM mice.

Group name	0 week (mmol/L)	1 week (mmol/L)	2 week (mmol/L)	3 week (mmol/L)	4 week (mmol/L)
CON	8.56±1.19	9.16±1.28	9.08±1.46	9.22±1.47	7.77±1.00
MOD	22.56±3.24$^{\#\#}$	27.78±3.43$^{\#\#}$	28.02±2.17$^{\#\#}$	27.57±2.18$^{\#\#}$	27.53±2.47$^{\#\#}$
MET	21.79±2.70	28.21±4.15	24.12±2.99**	24.02±2.80**	21.91±5.01**
KRS	21.86±3.10	25.03±3.25	27.00±3.99	24.95±2.57*	22.99±3.59**
PRO	21.20±2.77	25.88±2.05	25.71±3.49	26.89±2.13	23.81±2.82**
MIX	22.57±4.08	25.08±3.18	23.14±3.81**	24.02±4.38*	22.77±2.20**

Data are expressed as means ± standard deviation (n = 10). Asterisks indicate significant differences using Dunnett's test. *P < 0.05, **P < 0.01 (vs. MOD group). Hashes indicate significant differences using Dunnett's test. $^{\#}P$< 0.05, $^{\#\#}P$ < 0.01 (vs. CON group).

Figure S4. Evaluation of Lipid Profiles in T2DM Mice. (A) Levels of total cholesterol (TC) in each group of mice. (B) Levels of triglycerides (TG) in each group of mice. (C) Levels of low-density lipoprotein cholesterol (LDL-C) in each group of mice. (D) Levels of high-density lipoprotein cholesterol (HDL-C) in each group of mice. Data are expressed as means ± standard deviation (n = 10). Asterisks indicate significant differences using Dunnett's test. *P < 0.05, **P < 0.01 (vs. MOD group). Hashes indicate significant differences using Dunnett's test. $^{\#}P$< 0.05, $^{\#\#}P$ < 0.01 (vs. CON group).

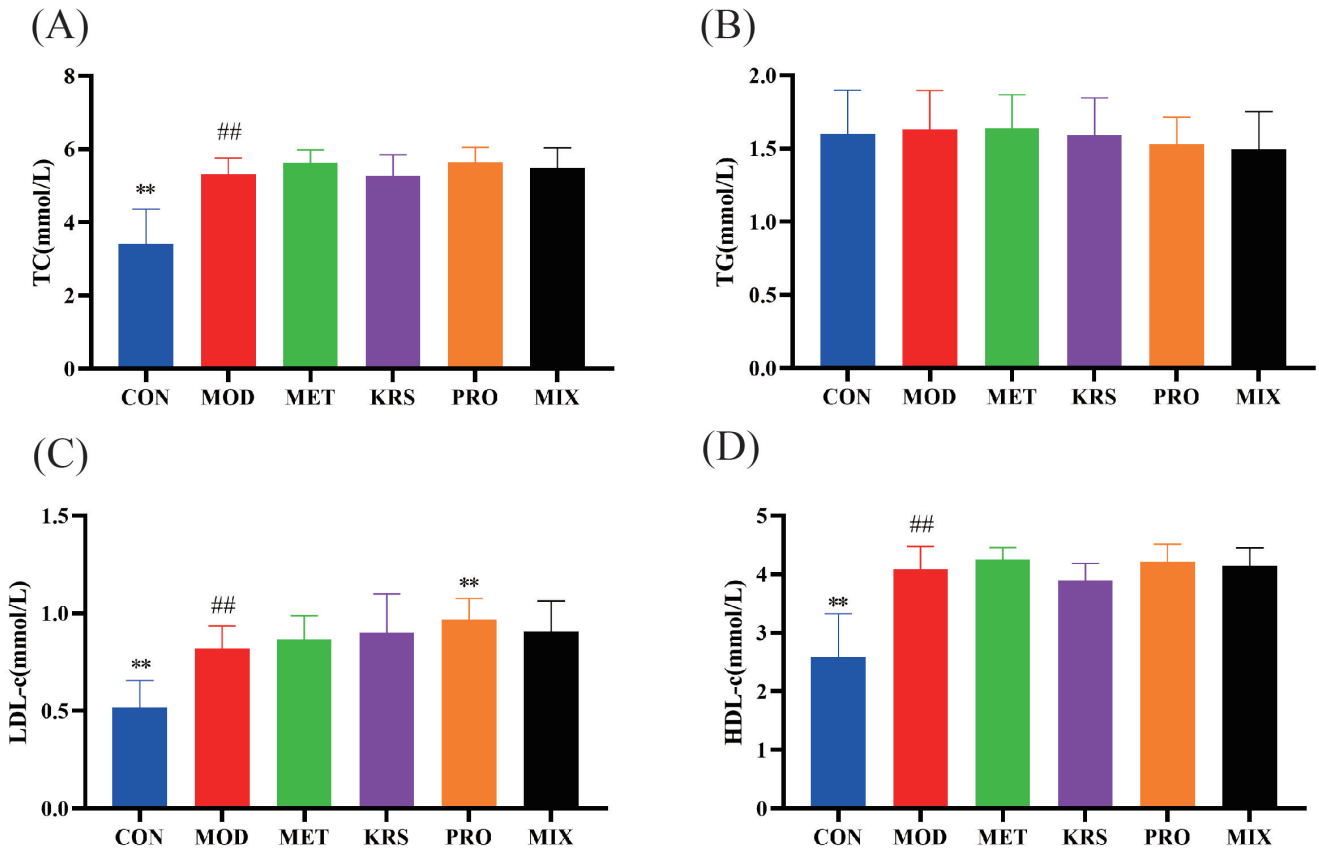

Figure 7. Comprehensive Assessment of Insulin Levels and Histopathological Changes in T2DM Mice. (B) Pancreatic H&E staining of each group of mice. (C) Levels of ALT and AST in each group of mice. (D) Hepatic H&E staining of each group of mice. Data are expressed as means ± standard deviation (n = 10). Asterisks indicate significant differences using Dunnett's test. *P < 0.05, **P < 0.01 (vs. MOD group). Hashes indicate significant differences using Dunnett's test. $^{\#}P$< 0.05, $^{\#\#}P$ < 0.01 (vs. CON group). Representative photomicrographs of H&E sections, scale bars: 50 μm.

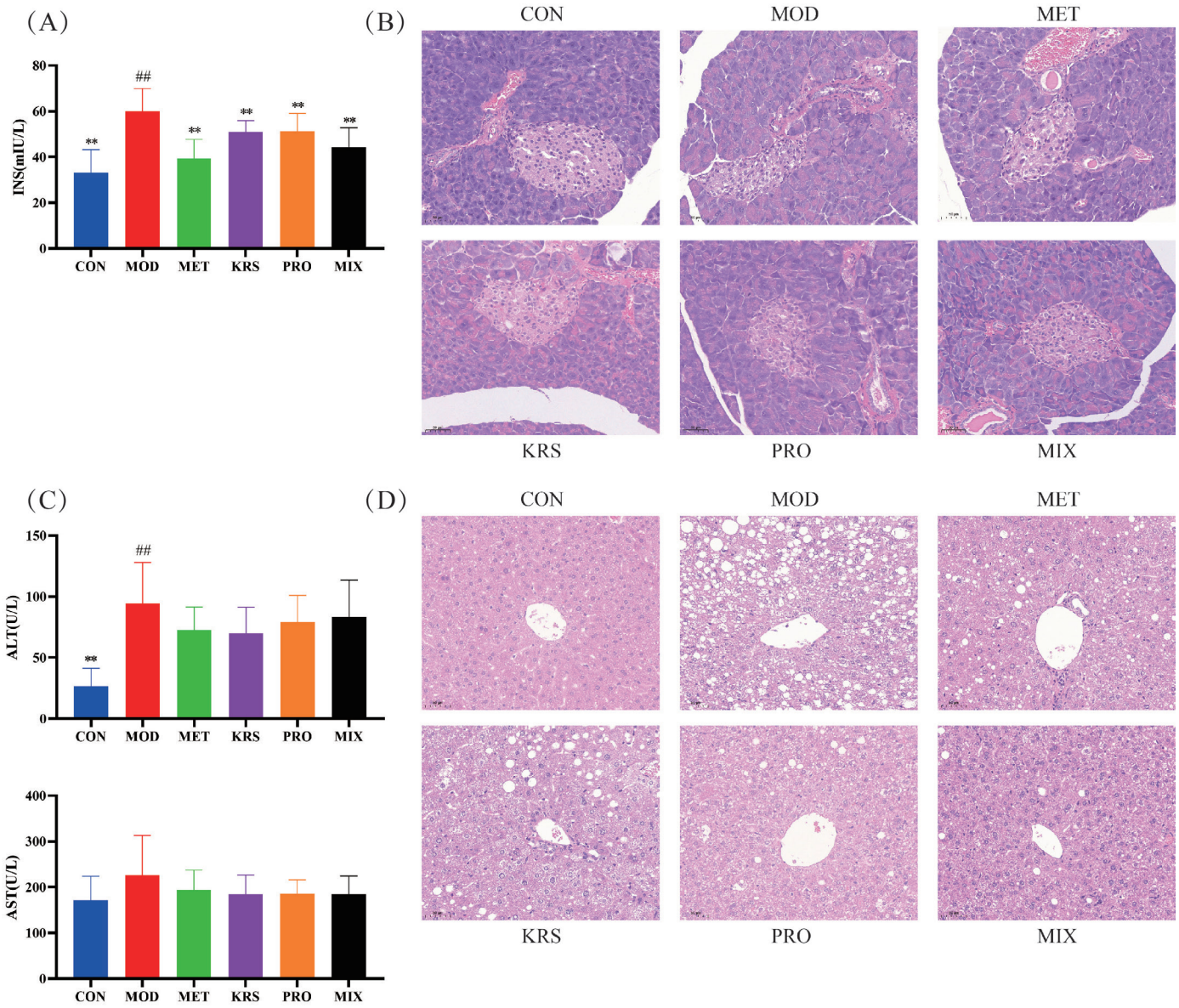

In addition to the above results, we measured the inflammatory indicators in T2DM mice. The levels of TNF-α, IL-1β, and IL-6 were significantly increased (P < 0.01), while the level of IL-10 was significantly decreased (P < 0.01) in MOD group, indicating that the T2DM model induced by a high-fat diet combined with STZ successfully triggered a chronic inflammatory response and caused an imbalance in inflammation. After intervention, compared with MOD group, the levels of TNF-α, IL-1β, and IL-6 decreased in all treatment groups, and the level of IL-10 significantly increased. The MET and MIX groups showed more pronounced effects **(Figure 8)**.

Figure 8. Evaluation of Inflammatory Profiles in T2DM Mice. (A) Levels of TNF-α in each group of mice. (B) Levels of IL-1β in each group of mice. (C) Levels of IL-10 in each group of mice. (D) Levels of IL-6 in each group of mice. Data are expressed as means ± standard deviation (n = 10). Asterisks indicate significant differences using Dunnett's test. *$P < 0.05$, **$P < 0.01$ (vs. MOD group). Hashes indicate significant differences using Dunnett's test. $^{\#}P < 0.05$, $^{\#\#}P < 0.01$ (vs. CON group).

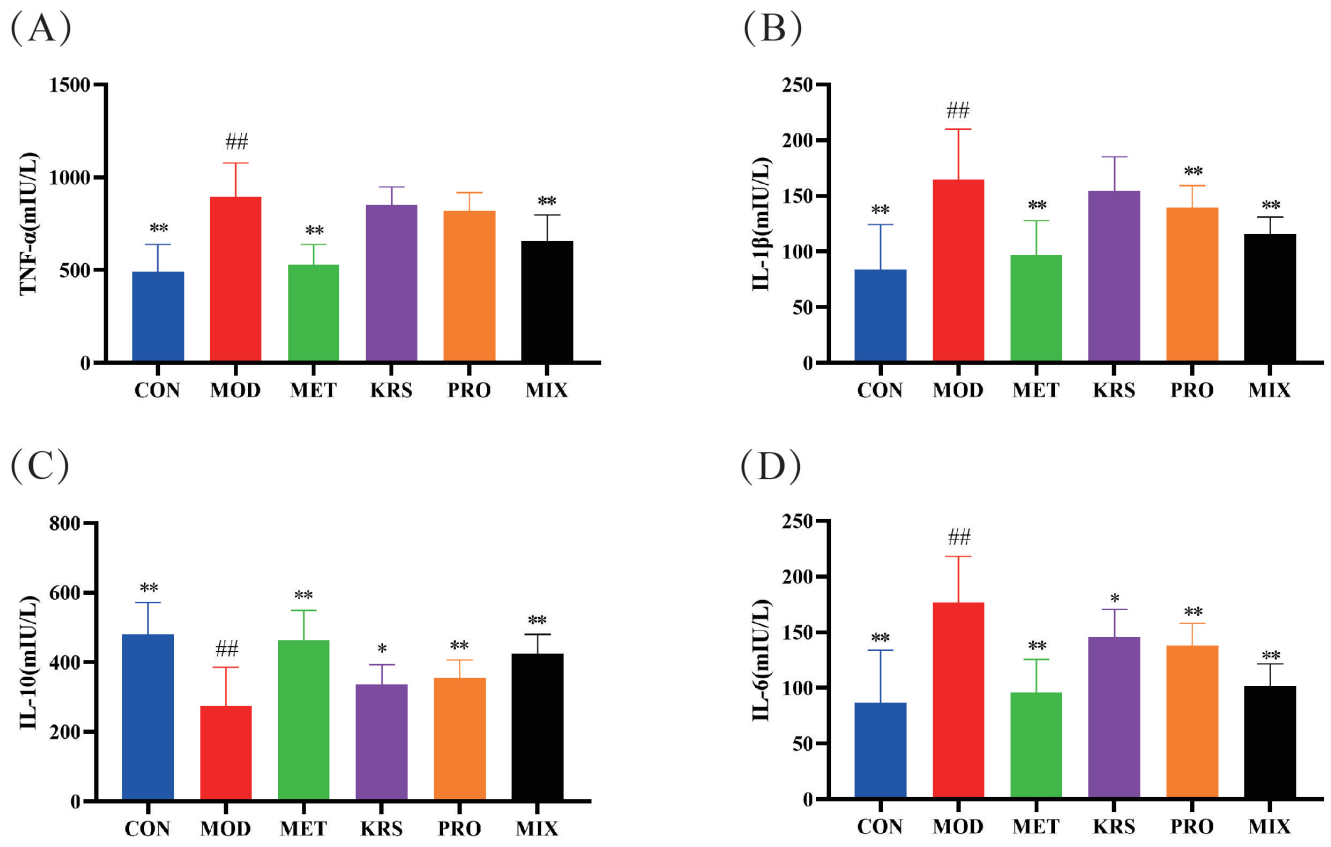

In terms of gut microbiota composition in mice, significant differences were observed among the intervention groups. MOD group showed decreased gut microbiota α-diversity compared to CON group. After intervention, KRS, PRO, and MIX groups exhibited increased Simpson and Shannon indices. In β-diversity analysis, the MOD group's gut microbiota structure differed significantly from CON group. The intervention groups' microbiota shifted significantly from MOD group along the PCoA2 axis and approached CON group **(Figure 9A-B)**.

Firmicutes and Bacteroidetes were the predominant phyla in the gut microbiota of mice, making up approximately 70% of the total relative abundance **(Figure 9C)**. These two phyla are the most common in the gut microbiota. Firmicutes, which mainly produce butyrate, are important for gut barrier function and energy metabolism. Bacteroidetes play a key role in carbohydrate degradation and fermentation, contributing to the production of short-chain fatty acids (SCFAs) and influencing gut health and host metabolism (32). In comparison to MOD group, KRS, PRO, and MIX groups had a notably higher relative abundance of *Actinobacteriota. Actinobacteriota*, though typically low in abundance, includes beneficial genera like *Bifidobacterium*, which regulate gut immunity, inhibit harmful bacteria, and improve gut barrier function (33). At the genus level, the top five most abundant microbes in the gut microbiota of mice were *un_f_Lachnospiraceae, Odoribacter, Muribaculaceae, Mucispirillum*, and *Helicobacter***(Figure 9D)**. Compared with MOD group, KRS, PRO, and MIX groups significantly enriched *un_f_Lachnospiraceae, Anaeroplasma*, and *Odoribacter***(Figure 10A)**. These genera are involved in SCFA production, gut barrier maintenance, and immune regulation. Specifically, *un_f_Lachnospiraceae* (a butyrate producer) is crucial for gut mucosal barrier function and immune regulation (34). *Anaeroplasma* may help modulate gut microbiota, while *Odoribacter* may improve gut metabolic functions (35). These changes reflect the significant impact of different treatments on gut microbiota structure and suggest potential mechanisms by which KRS, PRO, and MIX groups improve gut health and overall metabolic status. The results of LEfSe analysis **(Figure 10B)** revealed significant differences in the distribution of *Bifidobacterium* across different treatment groups. In KRS group, a slight increase in the relative abundance of *Bifidobacterium* was observed, further confirming the growth-promoting properties of KRS for this genus. The substantial enrichment of *Bifidobacterium* in PRO and MIX groups demonstrated its ability to colonize the mouse gut. This synergistic effect may involve inhibiting the proliferation of harmful

bacteria, strengthening the gut barrier, and modulating the host immune response. In contrast, CON, MOD, and MET groups exhibited extremely low levels of *Bifidobacterium*, which were almost undetectable. This may reflect the weak natural colonization ability of *Bifidobacterium* in the mouse gut microbiota without specific interventions, or that the treatment conditions of these groups were not conducive to the growth and maintenance of *Bifidobacterium*. In summary, the LEfSe analysis results suggest that KRS facilitates the enrichment of *Bifidobacterium* in mice, and *Bifidobacterium* administered via gavage can effectively colonize the mouse gut.

Figure 9. Diversity Analysis of Mice in Each Group. (A) α-diversity levels of mice in each group. (B) β-diversity levels of mice in each group. (C) Phylum-level composition of gut microbiota in different groups of mice. (D) Genus-level composition of gut microbiota in different groups of mice. Data are expressed as means ± standard deviation (n = 10).

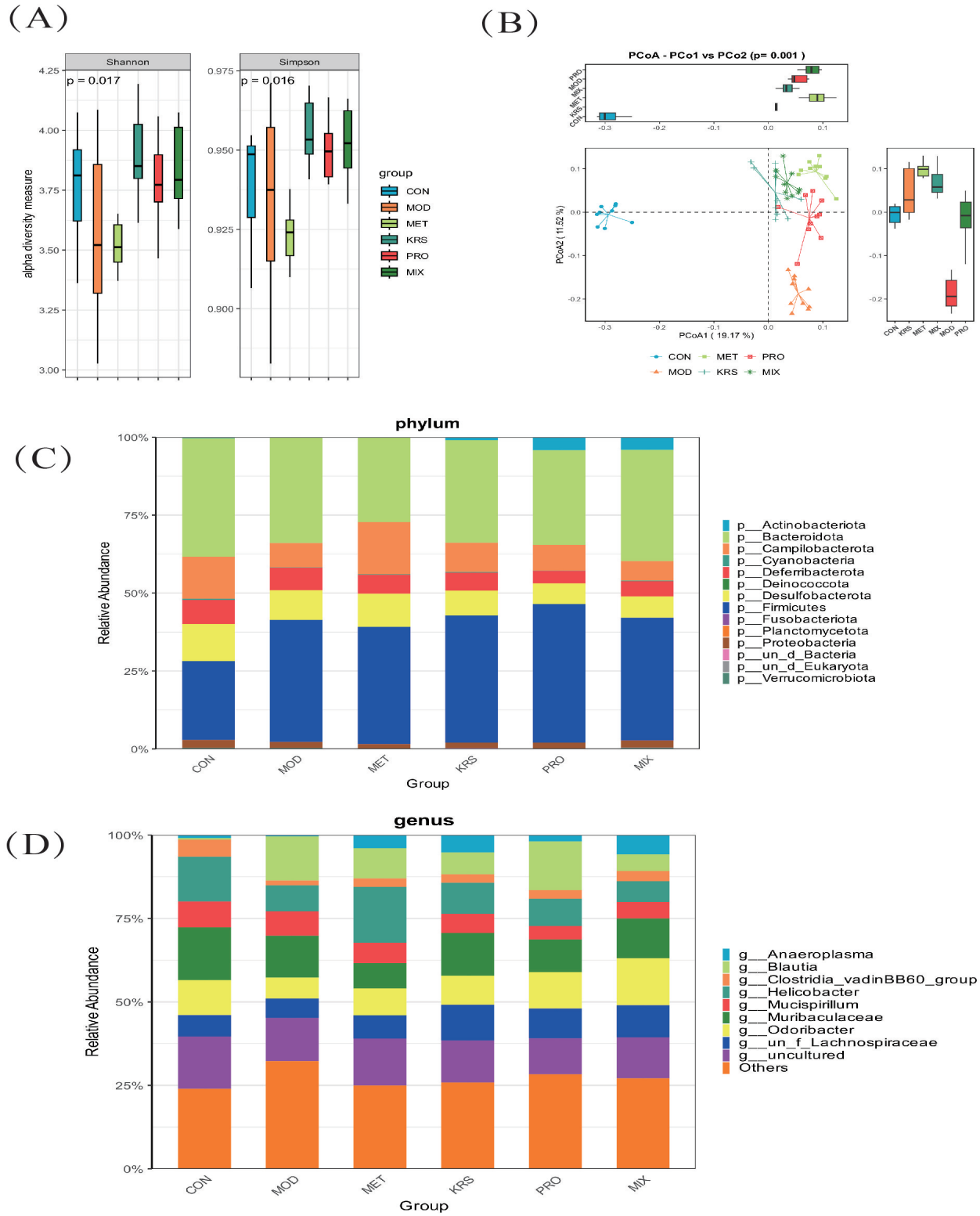

Figure 10. Effects of KRS on gut microbiota. (A) Differential analysis of gut microbiota at the genus level among different groups of mice. (B) Differential analysis of *Bifidobacterium* among different groups of mice. Data are expressed as means ± standard deviation (n = 10).

In the T2DM mouse model, the combined intervention of KRS and *Bifidobacterium adolescentis* TH02767 significantly improved body weight, blood glucose levels, glucose tolerance, and inflammatory responses in mice, while optimizing the structure and abundance of the gut microbiota. This synergistic effect suggests that the combination of KRS and probiotics may act through multiple mechanisms: on the one hand, KRS serves as a prebiotic to provide a growth substrate for beneficial bacteria; on the other hand, *Bifidobacterium adolescentis* TH02767 enhances host metabolic functions through its metabolic products. This combined intervention strategy not only improved glycemic control but also provided a more comprehensive solution for T2DM management by modulating the composition and function of the gut microbiota.

Despite achieving positive results in both *in vitro* and animal models, there are limitations to this study. For example, the experiments were conducted only in a T2DM mouse model induced by a high-fat diet combined with STZ, and the generalizability of the results needs to be further validated in more types of diabetes models. Additionally, the small sample size might influence the statistical significance of the findings. Future research should replicate the experiments with more animal models and larger sample sizes to confirm these results. Moreover, integrating multi-omics technologies, including metagenomics and metabolomics, could enhance our understanding of the mechanisms of KRS and probiotics, thereby supporting the development of novel functional foods and therapeutic strategies.

Acknowledgment

Ethics approval for the *in vitro* fecal fermentation was obtained from the Ethics Committee of the School of Medicine, Xiamen University (Ethics approval number: XDYX2022005). The animal experiments were approved by the Animal Ethics Committee of

the Second Affiliated Hospital of Fujian University of Traditional Chinese Medicine (Approval No.: FJPSPH-IAEC2024110).
This work was supported by the Natural Science Foundation of Fujian Province (Grant No. 2024J01232) and The National Natural Science Foundation of China (Grant No.U22A20376). We also thank Xiamen Treatgut Biotechnology Co. Ltd. for their technical support and assistance during the study.

Credit Authorship Contribution Statement

Wenting Jia: Writing e original draft, Methodology.
Shaojing Lin: Methodology.
Songjian Yuan: Methodology.
Haiyan Huang, Xiaomei Liu: Resources, Investigation.
Xiangman Ji: Resources, Investigation.
Bangzhou Zhang: Writing e review & editing.
Chuanxing Xiao: Writing e review & editing.

REFERENCES

1. Alberti, K. G. and Zimmet, P. Z.: Definition, diagnosis and classification of diabetes mellitus and its complications. Part 1: diagnosis and classification of diabetes mellitus provisional report of a WHO consultation. Diabet. Med. J. Br. Diabet. Assoc., 15, 539–553 (1998).

2. Du, Y. T., Rayner, C. K., Jones, K. L., Talley, N. J. and Horowitz, M.: Gastrointestinal Symptoms in Diabetes: Prevalence, Assessment, Pathogenesis, and Management. Diabetes Care, 41, 627–637 (2018).

3. Cho, N. H., Shaw, J. E., Karuranga, S., Huang, Y., da Rocha Fernandes, J. D., Ohlrogge, A. W. and Malanda, B.: IDF Diabetes Atlas: Global estimates of diabetes prevalence for 2017 and projections for 2045. Diabetes Res. Clin. Pract., 138, 271–281 (2018).

4. Lu, X., Xie, Q., Pan, X., Zhang, R., Zhang, X., Peng, G., Zhang, Y., Shen, S. and Tong, N.: Type 2 diabetes mellitus in adults: pathogenesis, prevention and therapy. Signal Transduct. Target. Ther., 9, 1–25 (2024).

5. Iatcu, C. O., Steen, A. and Covasa, M.: Gut Microbiota and Complications of Type-2 Diabetes. Nutrients, 14, 166 (2021).

6. Cole, J. B. and Florez, J. C.: Genetics of diabetes mellitus and diabetes complications. Nat. Rev. Nephrol., 16, 377–390 (2020).

7. Liu, L., Zhang, J., Cheng, Y., Zhu, M., Xiao, Z., Ruan, G. and Wei, Y.: Gut microbiota: A new target for T2DM prevention and treatment. Front. Endocrinol., 13, 958218 (2022).

8. Mondot, S., de Wouters, T., Doré, J. and Lepage, P.: The Human Gut Microbiome and Its Dysfunctions. Dig. Dis., 31, 278–285 (2013).

9. Arora, A., Behl, T., Sehgal, A., Singh, S., Sharma, N., Bhatia, S., Sobarzo-Sanchez, E. and Bungau, S.: Unravelling the involvement of gut microbiota in type 2 diabetes mellitus. Life Sci., 273, 119311 (2021).

10. Ma, Q., Li, Y., Li, P., Wang, M., Wang, J., Tang, Z., Wang, T., Luo, L., Wang, C., Wang, T. and Zhao, B.: Research progress in the relationship between type 2 diabetes mellitus and intestinal flora. Biomed. Pharmacother. Biomedecine Pharmacother., 117, 109138 (2019).

11. DeMartino, P. and Cockburn, D. W.: Resistant starch: impact on the gut microbiome and health. Curr. Opin. Biotechnol., 61, 66–71 (2020).

12. Prajapati, K., Bisani, K., Prajapati, H., Prajapati, S., Agrawal, D., Singh, S., Saraf, M. and Goswami, D.: Advances in probiotics research: mechanisms of action, health benefits, and limitations in applications. Syst. Microbiol. Biomanufacturing, 4, 386–406 (2024).

13. Zaman, S. A. and Sarbini, S. R.: The potential of resistant starch as a prebiotic. Crit. Rev. Biotechnol., 36, 578–584 (2016).

14. Sanchis-Chordà, J., del Pulgar, E. M. G., Carrasco-Luna, J., Benítez-Páez, A., Sanz, Y. and Codoñer-Franch, P.: *Bifidobacterium pseudocatenulatum* CECT 7765 supplementation improves inflammatory status in insulin-resistant obese children. Eur. J. Nutr., 58, 2789–2800 (2019).

15. Sabico, S., Al-Mashharawi, A., Al-Daghri, N. M., Yakout, S., Alnaami, A. M., Alokail, M. S. and McTernan, P. G.: Effects of a multi-strain probiotic supplement for 12 weeks in circulating endotoxin levels and cardiometabolic profiles of medication naïve T2DM patients: a randomized clinical trial. J. Transl. Med., 15, 249 (2017).

16. Song, X., Dong, H., Zang, Z., Wu, W., Zhu, W., Zhang, H. and Guan, Y.: Kudzu Resistant Starch: An Effective Regulator of Type 2 Diabetes Mellitus. Oxid. Med. Cell. Longev., 2021, 4448048 (2021).

17. Lian, Z., Xu, Y., Wang, C., Chen, Y., Yuan, L., Liu, Z., Liu, Y., He, P., Cai, Z. and Zhao, J.: Gut microbiota-derived melatonin from Puerariae Lobatae Radix-resistant starch supplementation attenuates ischemic stroke injury via a positive microbial co-occurrence pattern. Pharmacol. Res., 190, 106714 (2023).

18. Li, H., Zhang, L., Li, J., Wu, Q., Qian, L., He, J., Ni, Y., Kovatcheva-Datchary, P., Yuan, R., Liu, S., Shen, L., Zhang, M., and other 19 authors: Resistant starch intake facilitates weight loss in humans by reshaping the gut microbiota. Nat. Metab., (2024).

19. Qian, X., Si, Q., Lin, G., Zhu, M., Lu, J., Zhang, H., Wang, G. and Chen, W.: *Bifidobacterium adolescentis* Is Effective in Relieving Type 2 Diabetes and May Be Related to Its Dominant Core Genome and Gut Microbiota Modulation Capacity. Nutrients, 14, 2479 (2022).

20. Latif, A., Shehzad, A., Niazi, S., Zahid, A., Ashraf, W., Iqbal, M. W., Rehman, A., Riaz, T., Aadil, R. M., Khan, I. M., Özogul, F., Rocha, J. M., and other 4 authors: Probiotics: mechanism of action, health benefits and their application in food industries. Front. Microbiol., 14, 1216674 (2023).

21. Liu, J., Lin, H., Cao, M., Lin, T., Lin, A., Xu, W., Wang, H., He, J., Li, Y., Tang, H. and Zhang, B.: Shifts and importance of viable bacteria in treatment of DSS-induced ulcerative colitis mice with FMT. Front. Cell. Infect. Microbiol., 13, 1124256 (2023).

22. Lei, S., Li, X., Liu, L., Zheng, M., Chang, Q., Zhang, Y. and Zeng, H.: Effect of lotus seed resistant starch on tolerance of mice fecal microbiota to bile salt. Int. J. Biol. Macromol., 151, 384–393 (2020).

23. Chen, P., Zhang, Q., Dang, H., Liu, X., Tian, F., Zhao, J., Chen, Y., Zhang, H. and Chen, W.: Screening for potential new probiotic based on probiotic properties and α-glucosidase inhibitory activity. Food Control, 35, 65–72 (2014).

24. Kim, J.-S., Hyun, T. K. and Kim, M.-J.: The inhibitory effects of ethanol extracts from sorghum, foxtail millet and proso millet on α-glucosidase and α-amylase activitie. Food Chem., 124, 1647–1651 (2011).

25. Huang, Q., Chen, L., Teng, H., Song, H., Wu, X. and Xu, M.: Phenolic compounds ameliorate the glucose uptake in HepG2 cells' insulin resistance via activating AMPK: Anti-diabetic effect of phenolic compounds in HepG2 cells. J. Funct. Foods, 19, 487–494 (2015).

26. Amarnath, K., Narla, A. V., Pontrelli, S., Dong, J., Reddan, J., Taylor, B. R., Caglar, T., Schwartzman, J., Sauer, U., Cordero, O. X. and Hwa, T.: Stress-induced metabolic exchanges between complementary bacterial types underly a dynamic mechanism of inter-species stress resistance. Nat. Commun., 14, 3165 (2023).

27. Wang, L., Shang, Q., Guo, W., Wu, X., Wu, L., Wu, L. and Chen, T.: Evaluation of the hypoglycemic effect of probiotics via directly consuming glucose in intestines of STZ-induced diabetic mice and glucose water-induced diabetic mice. J. Funct. Foods, 64, 103614 (2020).

28. Zhao, M., Lu, C., Hu, X. and Ma, Z.: Evolution of multi-scale structure and microbiota metabolism of lentil resistant starch during the dynamic fermentation *in vitro*. Food Chem., 461, 140914 (2024).

29. Wang, X., Li, J., Shang, J., Bai, J., Wu, K., Liu, J., Yang, Z., Ou, H. and Shao, L.: Metabolites extracted from microorganisms as potential inhibitors of glycosidases (α-glucosidase and α-amylase): A review. Front. Microbiol., 13, (2022).

30. Cang, W., Li, X., Tang, J., Wang, Y., Mu, D., Wu, C., Shi, H., Shi, L., Wu, J. and Wu, R.: Therapeutic Potential of Bacteroides fragilis SNBF-1 as a Next-Generation Probiotic: *In Vitro* Efficacy in Lipid and Carbohydrate Metabolism and Antioxidant Activity. Foods Basel Switz., 13, 735 (2024).

31. Qu, Z., Liu, H., Yang, J., Zheng, L., Huang, J., Wang, Z., Xie, C., Zuo, W., Xia, X., Sun, L., Zhou, Y., Xie, Y., and other 9 authors: Selective utilization of medicinal polysaccharides by human gut *Bacteroides* and *Parabacteroides* species. Nat. Commun., 16, 638 (2025).

32. Pushpanathan, P., Mathew, G. S., Selvarajan, S., Seshadri, K. G. and Srikanth, P.: Gut microbiota and its mysteries. Indian J. Med. Microbiol., 37, 268–277 (2019).

33. Paul, P., Kaul, R., Harfouche, M., Arabi, M., Al-Najjar, Y., Sarkar, A., Saliba, R. and Chaari, A.: The effect of microbiome-modulating probiotics, prebiotics and synbiotics on glucose homeostasis in type 2 diabetes: A systematic review, meta-analysis, and meta-regression of clinical trials. Pharmacol. Res., 185, 106520 (2022).

34. Abdugheni, R., Wang, W.-Z., Wang, Y.-J., Du, M.-X., Liu, F.-L., Zhou, N., Jiang, C.-Y., Wang, C.-Y., Wu, L., Ma, J., Liu, C. and Liu, S.-J.: Metabolite profiling of human-originated *Lachnospiraceae* at the strain level. iMeta, 1, e58 (2022).

35. Leung, H. K. M., Lo, E. K. K., Zhang, F., Felicianna, Ismaiah, M. J., Chen, C. and El-Nezami, H.: Modulation of Gut Microbial Biomarkers and Metabolites in Cancer Management by Tea Compounds. Int. J. Mol. Sci., 25, 6348 (2024).